

PAPER

Porous $\text{SnO}_2\text{-Cu}_x\text{O}$ nanocomposite thin film on carbon nanotubes as electrodes for high performance supercapacitors

To cite this article: Farhad Daneshvar *et al* 2019 *Nanotechnology* **30** 015401

View the [article online](#) for updates and enhancements.



IOP | ebooks™

Bringing you innovative digital publishing with leading voices to create your essential collection of books in STEM research.

Start exploring the collection - download the first chapter of every title for free.

Porous SnO₂-Cu_xO nanocomposite thin film on carbon nanotubes as electrodes for high performance supercapacitors

Farhad Daneshvar¹ , Atif Aziz^{2,4}, Amr M Abdelkader³ , Tan Zhang¹, Hung-Jue Sue^{1,4} and Mark E Welland²

¹ Polymer Technology Centre, Department of Materials Science and Engineering, Texas A&M University, College Station, TX 77843, United States of America

² Nanoscience Centre, Department of Engineering, University of Cambridge, CB3 0FF, United Kingdom

³ Faculty of Science and Technology, Bournemouth University, Poole House, Talbot Campus, Poole, Dorset BH12 5BB, United Kingdom

E-mail: aa267@cam.ac.uk and hjsue@tamu.edu

Received 13 August 2018, revised 21 September 2018

Accepted for publication 2 October 2018

Published 25 October 2018



CrossMark

Abstract

Metal oxides are promising materials for supercapacitors due to their high theoretical capacitance. However, their poor electrical conductivity is a major challenge. Hybridization with conductive nanostructured carbon-based materials such as carbon nanotubes (CNTs) has been proposed to improve the conductivity and increase the surface area. In this work, CNTs are used as a template for synthesizing porous thin films of SnO₂-CuO-Cu₂O (SnO₂-Cu_xO) via an electroless deposition technique. Tin, with its high wettability and electrical conductivity, acts as an intermediate layer between copper and the CNTs and provides a strong interaction between them. We also observed that by controlling the interfacial characteristics of CNTs and varying the composition of the electroless bath, the SnO₂-Cu_xO thin film morphology can be easily manipulated. Electrochemical characterizations show that CNT/SnO₂-Cu_xO nanocomposite possesses pseudocapacitive behavior that reaches a specific capacitance of 662 F g⁻¹ and the retention is 94% after 5000 cycles, which outperforms any known copper and tin-based supercapacitors in the literature. This excellent performance is mainly attributed to high specific surface area, small particle size, the synergistic effect of Sn, and conductivity improvement by using CNTs. The combination of CNTs and metal oxides holds promise for supercapacitors with improved performance.

Supplementary material for this article is available [online](#)

Keywords: pseudocapacitance, carbon nanotube, copper oxide, electroless deposition, supercapacitor

(Some figures may appear in colour only in the online journal)

1. Introduction

Stringent environmental regulations, ever-increasing interest in electric vehicles (EVs), and their fast market growth, have enticed automotive companies to push for EVs sooner than anticipated. Extensive work on rechargeable batteries has

made this transition feasible. However, there are still significant obstacles to overcome. One of the deficiencies of rechargeable batteries occurs during acceleration of EVs when the battery is required to provide a huge amount of energy in a short period of time. This rapid energy depletion can damage the electrode materials, and reduce the battery's lifetime [1]. Therefore, there has been an effort to develop novel electrode materials with higher power density and

⁴ Authors to whom any correspondence should be addressed.

better stability [2, 3]. An alternative solution has been implemented: a complementary system alongside the battery, which has high cyclability and an ability to provide the demanded energy during acceleration [4, 5]. Supercapacitors or electrochemical capacitors (ECs) are an attractive option due to their high power density, long life span, high cyclic efficiency, safety and rapid charge–discharge rates [5–7].

Based on energy storage mechanisms, supercapacitors are categorized into two groups: electrical double layer capacitors and pseudocapacitors. The former purely works based on electron storage in a double layer while in the latter faradic redox reactions occur, which results in significantly higher specific capacitance and energy density [8, 9]. Pseudocapacitors typically are made of either polymers or transition metal oxides (TMOs). While polymers have good specific capacity and electrical conductivity, they suffer from poor cyclability due to substantial volume changes [10]. TMOs, on the other hand, generally possess higher specific capacitance, but their electrical conductivity is poor [11, 12]. Because pseudocapacitance relies on faradic reactions at the surface, a higher specific surface area provides more sites for metal oxide redox reactions, which improves the specific capacitance of the TMOs. In addition to specific surface area, electrical conductivity and microstructure also play major roles on capacitive behavior of TMOs.

Copper oxide is one of the promising TMOs for supercapacitor applications. It is an inexpensive and abundant material that possesses high theoretical capacity [13–15]. Therefore, recently these oxides, either in CuO or Cu₂O form, have attracted considerable interest as EC electrode material [14–20]. However, the electrochemical performance of these oxides suffers due to low conductivity and limited specific surface area [20, 21]. To tackle the obstacle of low electrical conductivity, hybridization with conductive carbon-based materials such as carbon black, graphene, or carbon nanotubes (CNTs) has been suggested [17, 22–26]. Among these, CNTs have attracted particular attention due to their high electrical conductivity, specific surface area, mechanical strength, electrochemical stability, and low electrical percolation threshold. As Liu *et al* [18] has shown, by introducing CNTs to electrode materials a conductive network is created which facilitates charge transfer through the electrode and enhances the specific capacitance of CuO nanosheets significantly.

However, progress in integrating CNTs in supercapacitors has been limited. For instance Zhang *et al* [23] observed that substituting CNT for carbon black as an additive in CuO electrode material did not significantly increase the specific capacitance (from 137 F g⁻¹ to 150 F g⁻¹). Nevertheless, previous research has shown that using CNTs during the synthesis of active material can yield advantages far beyond just forming a conductive network. In this case, CNTs can yield strong bonds with metal oxides by acting as supports or templates for nucleation and growth of active material. This not only enhances the charge transfer, but also results in size refinement, hinders agglomeration, and creates a coarse and mesoporous structure that results in higher

capacitance through easier charge transfer and higher specific surface area [25, 27–29].

In addition to hybridization with carbon nanostructures, hybridization with TMOs has shown to be a promising method for improving the electrochemical performance of electrodes in supercapacitors [29–32]. For instance, Sugimoto *et al* [31] reported that by introducing VO₂ to RuO₂ the specific surface area was tripled and the specific capacitance reached 1210 F g⁻¹, which exceeds that of an Ru₂O electrode by 60%. In addition to increasing the surface area, doping a secondary oxide can improve the electrochemical performance by enhancing the conductivity, uniformly dispersing the active material or refining the particle size. Stannic oxide is one of the oxides that has been studied as an additive in composite electrodes. SnO₂ not only has the conventional redox properties, but also is inexpensive, has high wettability, and relative to other TMOs, has higher electronic conductivity [5]. It has been observed that adding SnO₂ has a synergistic effect on electrode performance, especially through increasing electrical conductivity and facilitating electron and proton conduction [32]. Therefore, regardless of the material type, by choosing a suitable additive the electrochemical performance of the electrode can be enhanced.

In this work multi-walled CNTs (MWCNTs) were used as a template for the growth of tin and copper oxide (CuO_x-SnO₂) nanoparticles using electroless deposition (ED). ED is a simple and scalable technique that provides morphology control by easily changing the parameters, such as pH and bath composition, and can produce rough and porous structures [33, 34]. Moreover, by using MWCNTs we were able to engineer the morphology of SnO₂-Cu_xO thin film in nanoscale and create a one-dimensional (1D) porous structure that offers high surface area and short transport/diffusion pathways for electrons/ions, which leads to fast kinetics and high capacity. Strong bonding between the thin film and MWCNTs and the 1D porous SnO₂-Cu_xO structure provides an excellent cycle stability through accommodating the volume changes caused by faradic reactions. Electrochemical tests have shown that deposition of tin and copper oxides on CNTs can result in a hybrid material that outperforms any reported copper-based and tin-based supercapacitors in the literature with respect to specific capacitance and cyclability (table S1 is available online at stacks.iop.org/NANO/30/015401/mmedia).

2. Experimental procedure

2.1. Materials and methods

MWCNTs with a purity of 95 wt%, diameter of 20–40 nm and length of 10–30 μm were supplied by Arkema Inc. All other chemicals were obtained from Sigma-Aldrich and were used as-received. For obtaining a good dispersion they were exfoliated according to a previous report [35]. Briefly, 250 mg as-received MWCNTs were added to a mixture of H₂SO₄ (45 ml) and HNO₃ (15 ml) in a 3:1 volume ratio. This mixture

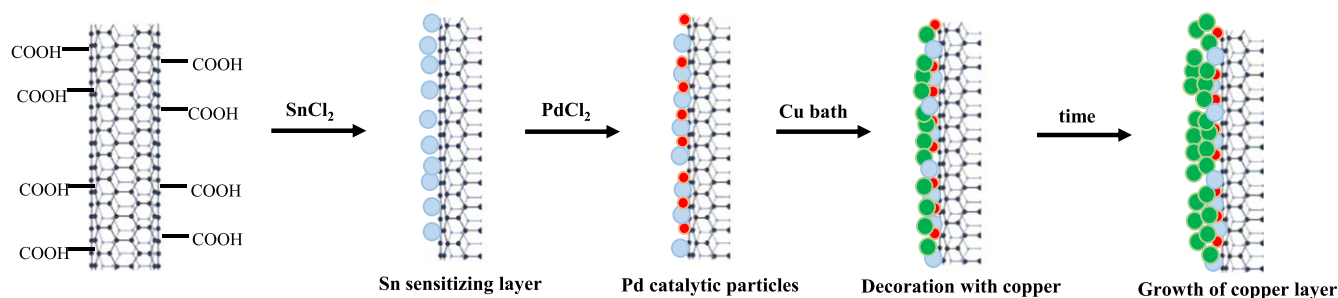


Figure 1. A schematic of an electroless deposition process on CNTs. Blue, red and green spheres represent Sn, Pd and Cu particles respectively.

Table 1. Chemical composition of copper electroless bath.

Chemical composition	Quantity
CuSO ₄ ·5H ₂ O	6.2 g l ⁻¹
2Na-EDTA	40 g l ⁻¹
Na ₂ SO ₄	35 g l ⁻¹
HCOONa	60 g l ⁻¹
CHOH (37 vol% in water)	20 ml l ⁻¹
Temperature	60 °C
pH (NaOH)	13

was sonicated in a sonication bath for two hours at 25 °C [36] and then washed with DI water.

Synthesis of SnO₂-Cu_xO/CNT hybrid structure by ED consists of several steps, which are schematically represented in figure 1. First, 50 mg of oxidized MWCNTs were added to a 50 ml aqueous solution of SnCl₂ (0.98 g) and 0.1 ml HCl (37 wt%). The mixture was sonicated for 15 min, and then washed with DI water. CNTs usually have weak interactions with metallic particles. In supercapacitor applications this can result in lower conductivity and detachment of metal oxides from the CNTs. Tin has a high wetting capability and therefore readily attaches to the surface of MWCNTs. The tin layer will act as an intermediate layer for adsorption of other metallic-based particles during the following processing steps. In the next step, sensitized MWCNTs are added to a 50 ml DI water solution containing 0.007 g PdCl₂ and 0.1 ml HCl (37 wt%) and sonicated for 15 min. During this stage (i.e. activation), palladium ions replace a portion of the tin particles on the surface of MWCNTs and act as catalysts for nucleation and growth of copper. Finally after washing with DI water, activated MWCNTs are dispersed in a 50 ml copper ED bath with the chemical composition presented in table 1. After 15 min of stirring at 60 °C, 0.2 ml formaldehyde solution was added gradually to reduce the copper ions. After 30 min of stirring at 60 °C copper coated MWCNTs were washed and separated by centrifuge.

2.2. Characterization

For assessing the coating morphology a TEM (FEI Teccai G2 S-Twin, Philips) was used. The crystallographic phases of all of the samples were investigated using an XRD (Bruker D8 Advance ECO) with CuK_α incident radiation ($\lambda = 0.1506$ nm).

XPS was obtained from an Omicron DAR 40 dual Mg/Al x-ray source for XPS measurements and the HIS 13 He UV source for UPS measurements. STEM and EDX images were obtained using a FEI Tecnai Osiris S/TEM working at 200 keV. The EDX detectors were FEI Super-X systems employing 4 Bruker silicon drift detectors for high collection efficiency (>0.9 sr solid angle) and high count rates (>250 kcps).

2.3. Electrochemical tests

The electrochemical performance of the supercapacitors were tested in a conventional three-electrode (versus Ag/AgCl) and two electrode coin cells. All the electrochemical measurements, including cyclic voltammetry and galvanostatic charge/discharge, were conducted using an Iviumstat Electrochemical Interface. Cyclic voltammetry tests were carried out with the two electrode cells. Electrodes were prepared by mixing the hybrid material with poly-vinylidene fluoride and carbon black (80:10:10 in mass ratio) using a pestle and mortar. Cyclic voltammetry (CV) measurements were recorded in a 6 M KOH aqueous electrolyte in the range of -0.4 to 0.4 V at different scan rates.

3. Results and discussion

The chemical composition of the hybrid system was investigated using XPS, XRD and EDX. Figure 2(a) represents the XPS spectrum where the peaks at binding energies of 284.4, 486.5 and 933.9 eV correspond to C 1s, Sn 3d and Cu 2p, respectively. The C 1s peak is associated with the sp² C-C bond of MWCNTs and can be deconvoluted into C=C at 284.3 eV, and C-O at 285.8 eV and C=O at 288.2 eV [37–39]. The presence of these peaks underneath the C 1s is an indication of functional groups on the surface of MWCNTs created during acid treatment. These groups not only enhance the bonding between the metal oxides and MWCNTs, but also increase the wettability and hydrophilicity of the hybrid system, which helps to increase electrolyte ion transport within the structure. Moreover, Pan *et al* [40] observed redox peaks in CV curves of functionalized CNTs, indicating that these oxygenated groups on the surface may induce faradic redox reactions, which can enhance the specific capacitance. Finally, it should be noted that proper acid treatment can increase the specific surface area of

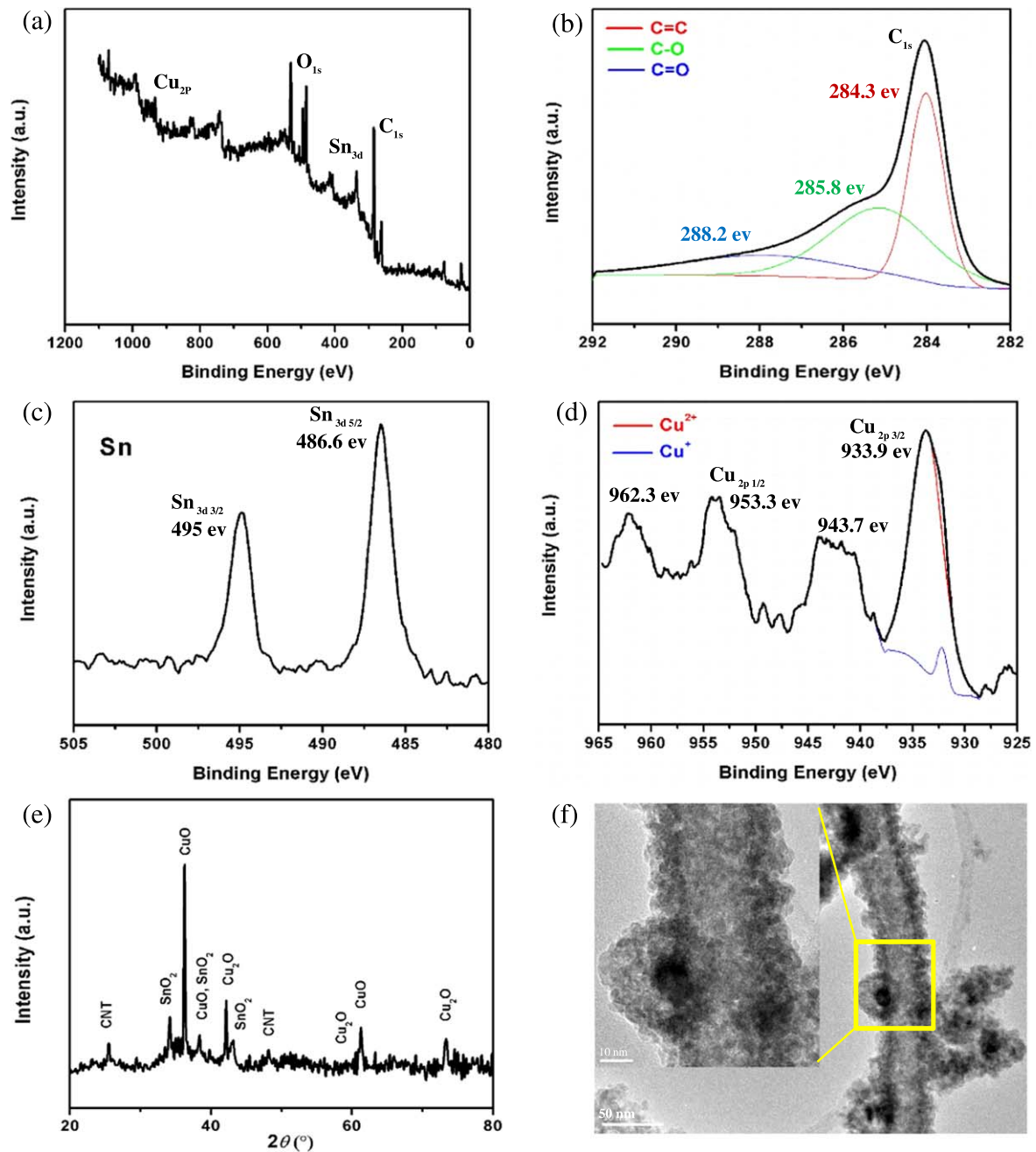


Figure 2. XPS spectra of (a) a hybrid system, (b) C 1s of CNT, (c) Sn 3d of SnO₂, (d) Cu 2p spectrum of CuO/Cu₂O, (e) XRD of the hybrid sample and (f) TEM images of coated CNTs. The scale bar in the intersected picture is 10 nm.

MWCNTs either by creating defects at the surface or dissolving the catalysts and opening the tube ends. As a result, due to capillary forces during ED process, metallic ions can diffuse and deposit inside the tube.

The peaks relating to Sn are situated at 495 eV and 486.6 eV belonging to Sn 3d_{3/2} and Sn 3d_{5/2}, respectively. These results are identical to the reference data for Sn 3d in SnO₂ [41]. As represented in figure 2(d), the high-resolution XPS spectra for Cu consist of four peaks. The peaks observed at 933.9 eV and 953.3 eV are attributed to Cu 2p_{3/2} and Cu 2p_{1/2}, respectively [42]. Moreover, two strong satellite peaks are seen at higher binding energies compared to the main

peaks: a sharp peak at 962.35 eV and a broad peak between 941 to 945 eV. The overall spectrum is similar to CuO. However, by analyzing the main Cu 2p_{1/2} peak more carefully, it can be noted that at lower binding energies another peak exists; therefore, the Cu 2p_{3/2} peak can also be deconvoluted into two peaks by the Gaussian method. The new peak at lower binding energy (932.3 eV) has a low intensity and is characteristic of Cu₂O [43, 44], confirming that CuO and Cu₂O oxides coexist in the deposited coating, which is in accordance with the XRD results (figure 2(e)).

The morphology and microstructure of the hybrid system is represented in figure 2(f). It can be observed that the

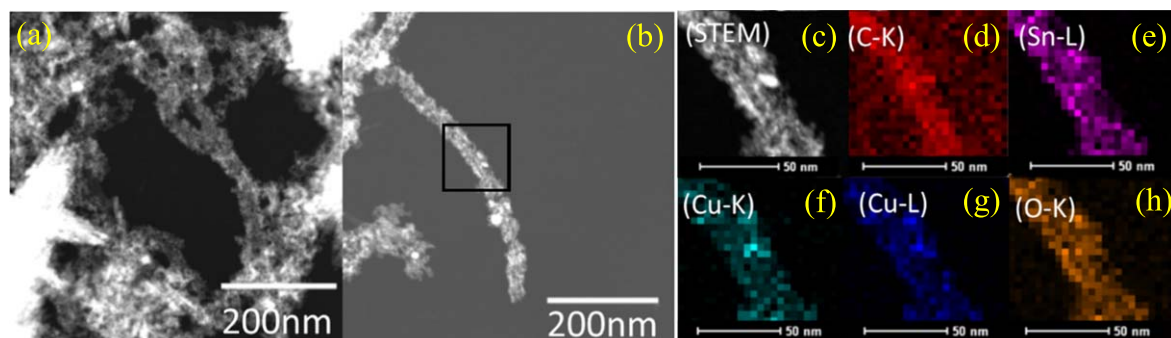
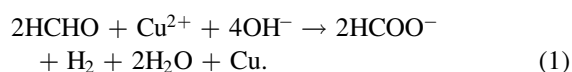


Figure 3. STEM (a)–(c) and EDX (d)–(h) of an electroless coated representative CNT. The black box shows the location where the elemental map was obtained.

coating has a rough surface in nanoscale and contains pores less than 1 nm in size, which makes this structure suitable for aqueous electrolytes [6]. Also, the thickness of the coating is generally 10–15 nm. Such a fine and porous structure provides a large accessible surface area and facilitates electrolyte penetration [2]. As a result most of the nanocomposite can take part in faradic reactions, which has a positive effect on capacitance.

From STEM images and nanoscale elemental maps (figure 3) of the electroless deposited MWCNT, it is observed that the tube is present at the core and is uniformly covered with tin and copper oxides. Images with lower magnification (figure S2) show that some of the MWCNTs are completely and some partially covered with metal oxide layer (the effect of coating density will be discussed). No observable x-ray signal was seen from palladium, which could be due the fact that it was completely covered by the Cu layer and the quantity was too small to be detectable.

As can be observed in figures 2(f) and 3, MWCNTs act as a template for deposition of fine copper nanoparticles and create a core–shell structure [45]. The C–OH and C=O bonds created during the acid treatment provide sites for adsorption of Sn/palladium ions. Since these defects eventually act as nucleation sites for copper, it is expected that application of functionalized MWCNTs also plays a major role in size refinement and morphology control [28]. The adsorbed Pd/Sn nuclei subsequently act as a catalyst for reduction and nucleation of copper according to the following reaction [46]:

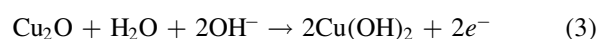
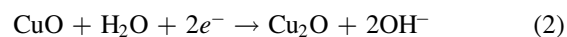


It should be noted that the produced copper in particles are in nanoscale therefore dissolved oxygen in water readily oxidizes the Cu and Sn particles. This can lead to finer particle size since copper growth favorably occurs on the fresh copper nuclei and oxidation hinders copper particle growth.

Using a MWCNT backbone structure not only improves the electrical conductivity but also increases the surface area. As can be seen in figure 2(f), deposited metal oxides adopt the 1D structure of MWCNTs and the maximum thickness reaches 15 nm. By considering the porous structure of the thin film, we can assume that most of metal oxides are accessible

by the electrolyte. Moreover, assembling these 1D hybrid structures of $\text{SnO}_2\text{-Cu}_x\text{O/CNT}$ creates a three-dimensional (3D) porous conductive network, which further enhances the electrolyte accessibility and promotes both electron and ion transport within the electrode material. Furthermore, we observed that the morphology, density and size of deposited particles are affected by the MWCNT surface modification method. If the oxidation of CNTs is not sufficient, the coating will be scarce (as shown in the supplementary information S1). It should be noted that if the MWCNTs are fully coated with a thick layer of metal oxide, the conductivity of the hybrid system, and as a result the capacitance of the electrode, reduces [47]. It should be added that before performing TEM analysis, the sample was diluted in water and went through a sonication step. The fact that the coating is still attached after the sonication process shows that there is a strong interaction between the MWCNT and copper coating, which can help to preserve the integrity of the electrode through charge–discharge cycles and enhance the capacitance performance of the hybrid material [47–49].

The electrochemical performance of the supercapacitor electrode was assessed by CV and galvanostatic charge/discharge tests in a two electrode coin cell configuration. Figure 4(a) shows the CV curves of the MWCNT and the $\text{SnO}_2\text{-Cu}_x\text{O/CNT}$ electrodes at scan rate 5 mV s^{-1} using a potential window from -0.4 V to 0.4 V in 6 M KOH solution. The CV curves of pure MWCNT show a nearly rectangular shape without any obvious redox peaks, indicating that the capacitance primarily originates from the double layer capacitance. By utilizing $\text{SnO}_2\text{-Cu}_x\text{O/CNT}$ as the electrode, two distinct reduction peaks and one oxidation peak were observed. While the observation of the redox peaks is a sign of pseudocapacitance contribution. The background current is significantly higher for $\text{SnO}_2\text{-Cu}_x\text{O/CNT}$ than for MWCNT, which couples with the rectangular shape of the CV curve, suggesting a double layer capacitance contribution from the copper oxide coating on MWCNTs. The pseudocapacitance behavior in the CV scans is associated with the following reactions [14, 50, 51]:



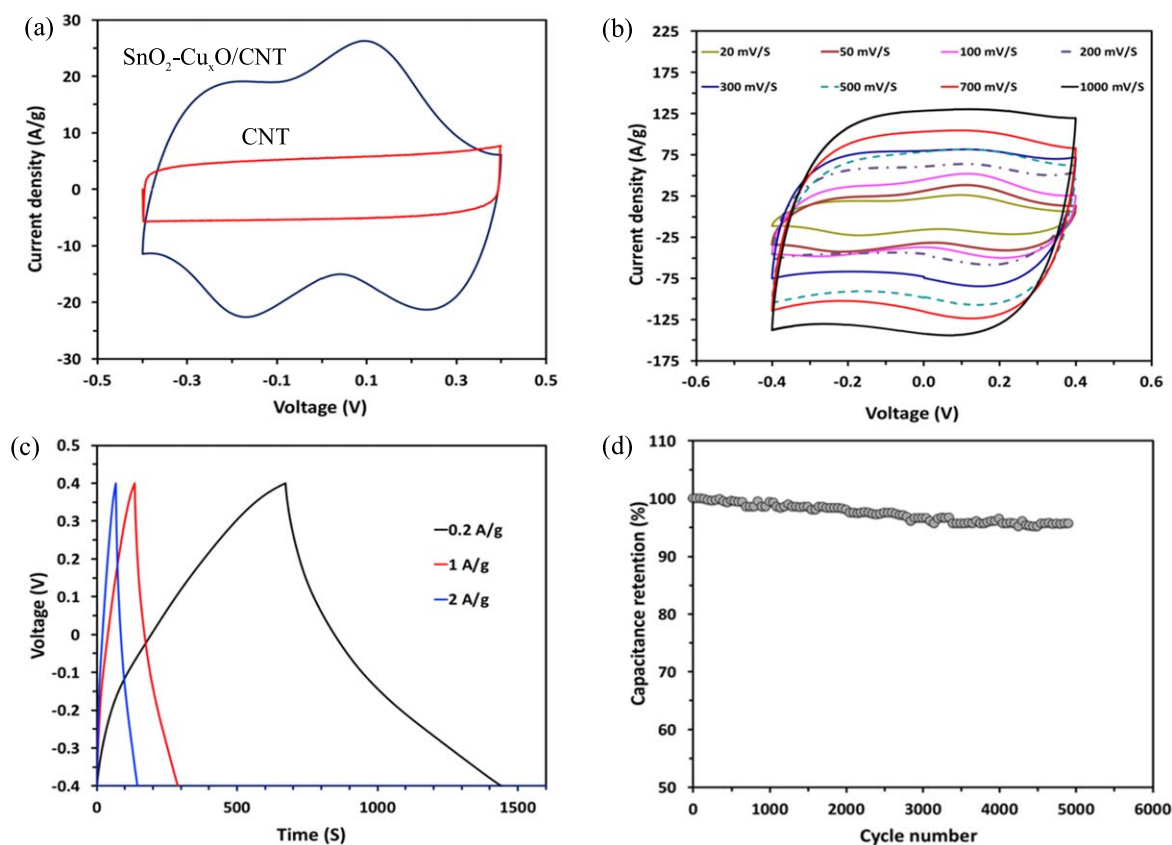
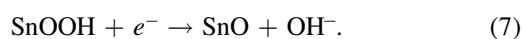
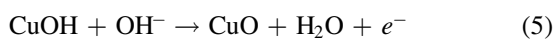


Figure 4. The electrochemical performance of the SnO₂-Cu_xO/CNT electrode: (a) CV of CNT and electroplated CNT electrode at 5 mV S⁻¹, (b) CV of the electroplated electrode at different scan rate, (c) charge-discharge curve at different current density, and (d) cycling performance at current density of 1 A g⁻¹.



One anodic peak and two cathodic peaks are observed in the operated potential range. The anodic peak can be ascribed to the oxidation of either Cu₂O or CuOH to CuO and/or Cu(OH)₂. It is possible that these two peaks have overlapped with each other. The cathodic peaks are attributed to the reduction of CuO and/or Cu(OH)₂ to Cu₂O and/or CuOH [14, 50]. It should be noted that based on the previous works in this potential range SnO₂ does not show clear redox peaks [51–55] therefore it can be concluded that the overall shape of the CV curve is dominated by copper oxide performance. Also it has been reported before that the pseudocapacitance contribution of CuO is mainly governed by the reduction of Cu²⁺ to Cu⁺ in KOH solutions [3, 56, 57]. Detecting two reduction peaks in the current study suggests that copper ions exist in two oxidation states, which is in agreement with XPS results. It is possible that the presence of carbon stabilizes the Cu⁺ oxidation states. In the early stages of the ED process it was observed that if the tube ends are open due to capillary forces, tin and copper deposit inside the MWCNTs (figure S4). These well-defined and narrow channels inside CNTs possess unique electronic

properties that make the confined metal oxide particles stay in a more reduced state. This phenomenon has been previously reported for some metal oxides such as manganese [58], tin [59], and iron [60]. This confinement can enhance the capacitance of the nanocomposite electrode; due to curvature, π -electron is denser at the outer surface of the CNT, which leads to electron deficiency inside the interior hollow cavity of CNTs. As a result the charge transfers from electron donor metal oxide to compensate for the electron deficiency inside the nanotube. This is helpful in the adsorption-desorption process of positive ions in the electrolyte such as K⁺ and H⁺ [58, 59] and enhance the capacity. Also the density functional theory calculations of Ng *et al* [61] and experimental works on confined Sn particles within CNTs [59] have shown that CNTs with encapsulated Sn have higher electrical conductivity compared with standalone CNTs, which also can enhance the capacitance.

The capacitance performance of the core-shell structure was evaluated with cyclic voltammograms in a scan rate range of 20 to 1000 mV s⁻¹. As it can be observed in figure 4(b), with increasing scan rate, the redox peaks almost vanish, and the CV curves of the hybrid system become featureless, suggesting the faradic reactions are diffusion limited. The CV curve, however, maintains a nearly rectangular and good mirror

images of the zero-current line even at high scan rates indicate an ideal capacitive behavior [19].

We have also used galvanostatic charge/discharge analysis for practical evaluation of the SnO₂-Cu_xO/CNT electrode capacitance in an alkali electrolyte (figure 4(c)). The curve for the MWCNT is nearly triangular and shows linear charge and discharge profiles, indicating purely capacitive behavior [62]. The SnO₂-Cu_xO/CNT shows a pair of bending points at potentials close to those in the CV curve. In both cases, the charge/discharge curves were symmetrical, indicating good electrochemical capacitive characteristics and excellent reversible redox reaction. Interestingly, the SnO₂-Cu_xO/CNT electrode displays almost no drop in internal resistance (IR) at the beginning of the discharge curve, indicating low overall IR of the nanocomposite electrode. The corresponding specific capacitance was calculated from the slopes of the discharge branch of the curve using the following equation:

$$C_s = \frac{4i}{-\frac{\Delta V}{\Delta t}m} = \frac{4i}{-slope \times m} \quad (8)$$

in which i is the current applied, $\Delta V/\Delta t$ is the slope of the discharge curve, and m is the mass of the nanocomposite electrode. The SnO₂-Cu_xO/CNT electrode can reach a specific capacitance as high as 662 F g⁻¹ at 0.2 A g⁻¹. To our knowledge, this value is the highest reported in the literature for a CuO based capacitor (about 569 F g⁻¹ and 545 F g⁻¹ for binder free CuO nanosheets on Ni foam at similar scan rates) [15, 63]. The supercapacitor electrode was cycled for 5000 cycles and retained about 94% of its initial capacitance (figure 4(d)), which is much superior compared to previous results [15, 63]. The excellent cyclability performance is attributed to the 1D porous structure and strong bonding between the constituents of the nanocomposite. 1D porous structure provides space for accommodating the volume changes during charge-discharge cycles. Strong bonding between the metal oxides and MWCNTs helps to preserve the integrity of the electrode material. In this regard tin's role is very crucial. It has relatively high electrical conductivity and excellent wettability. It readily adheres to the MWCNTs surface and makes it suitable for nucleation and growth of copper particles. Because copper is directly nucleated on tin, a strong interaction between these two components exists. Therefore tin oxide acts as an intermediate layer between copper oxide and the MWCNTs. In addition, using tin oxide can have other synergistic advantages, i.e. particle size refinement and enhancement of electronic and redox properties of the electrode material [32, 64].

To summarize, the improved performance of the SnO₂-Cu_xO/CNT electrode can be attributed to the following aspects: (i) abundant void space between the porous nanostructures not only provide short distance for the diffusion of the electrolyte but also offer a large number of electroactive sites for faradaic redox reactions to take place, hence improving the pseudocapacitive performance, (ii) the 3D

carbon network works as the backbone that provides mechanical integrity and facilitates electronic transportation within the electrodes, (iii) SnO₂ has a synergistic effect on Cu_xO performance through wetting the surface of MWCNTs, modifying the particle size and enhancing the conductivity of the nanocomposite, (iv) by acid treatment the ends of MWCNTs open, which results in infiltration and capsulation of metal oxide particles inside the MWCNT. These confined particles possess higher conductivity, smaller particle size and can facilitate diffusion of ions in the electrolyte, which leads to higher capacitance, and (v) anchoring the CuO_x nanoparticles, which minimizes aggregation and maximizes high specific surface area.

4. Conclusion

Three-dimensional network of a SnO₂-Cu_xO/CNT wire structure with MWCNTs as the substrate and copper oxide as the coating were synthesized through an electroless deposition technique. This facile and controllable processing method produces a unique core-shell structure with high porosity that enables fast ion and electron transports. The copper oxide nanoparticles enhance the capacitance through additional faradic redox reactions. The new hybrid shows excellent electrochemical performance as a supercapacitor electrode with a specific capacity of 662 F g⁻¹. The electrode is robust and capable of retaining more than 94% of its original capacity after 5000 cycles, indicating excellent electrochemical stability. Such an outstanding performance suggests that by engineering the CNT surfaces and utilizing the ED method, high capacity energy storage materials can be produced. Moreover, this method can be easily applied to other metal oxides to produce high performance supercapacitor electrodes.



Acknowledgments

All the authors acknowledge the support of the Lloyd's Register Foundation, London, UK, who has funded this research through their grants to protect life and property by supporting engineering-related education, public engagement and the application of research.

Conflict of interest

There are no conflicts to declare.

ORCID iDs

Farhad Daneshvar  <https://orcid.org/0000-0002-4105-5329>
Amr M Abdelkader  <https://orcid.org/0000-0002-8103-2420>

References

- [1] Peterson S B, Apt J and Whitacre J 2010 Lithium-ion battery cell degradation resulting from realistic vehicle and vehicle-to-grid utilization *J. Power Sources* **195** 2385–92
- [2] Simon P and Gogotsi Y 2008 Materials for electrochemical capacitors *Nat. Mater.* **7** 845
- [3] Ameri B, Davarani S S H, Roshani R, Moazami H R and Tadjarodi A 2017 A flexible mechanochemical route for the synthesis of copper oxide nanorods/nanoparticles/nanowires for supercapacitor applications: the effect of morphology on the charge storage ability *J. Alloys Compd* **695** 114–23
- [4] Pay S and Baghzouz Y 2003 Effectiveness of battery-supercapacitor combination in electric vehicles *IEEE Bologna Power Tech Conf. Proc* vol 3 (23–26 June 2003) (IEEE) DOI: [10.1109/PTC.2003.1304472](https://doi.org/10.1109/PTC.2003.1304472)
- [5] Wang G, Zhang L and Zhang J 2012 A review of electrode materials for electrochemical supercapacitors *Chem. Soc. Rev.* **41** 797–828
- [6] Simon P, Gogotsi Y and Dunn B 2014 Where do batteries end and supercapacitors begin? *Science* **343** 1210–1
- [7] Abdelkader A M 2015 Electrochemical synthesis of highly corrugated graphene sheets for high performance supercapacitors *J. Mater. Chem. A* **3** 8519–25
- [8] Zhang Y, Li L, Su H, Huang W and Dong X 2015 Binary metal oxide: advanced energy storage materials in supercapacitors *J. Mater. Chem. A* **3** 43–59
- [9] Hao P, Tian J, Sang Y, Tuan C-C, Cui G, Shi X, Wong C, Tang B and Liu H 2016 1D Ni-Co oxide and sulfide nanorod/carbon aerogel hybrid nanostructures for asymmetric supercapacitors with high energy density and excellent cycling stability *Nanoscale* **8** 16292–301
- [10] Snook G A, Kao P and Best A S 2011 Conducting-polymer-based supercapacitor devices and electrodes *J. Power Sources* **196** 1–12
- [11] Wu Z, Zhu Y and Ji X 2014 NiCo₂O₄-based materials for electrochemical supercapacitors *J. Mater. Chem. A* **2** 14759–72
- [12] Jiang J, Li Y, Liu J, Huang X, Yuan C and Lou X W 2012 Recent advances in metal oxide-based electrode architecture design for electrochemical energy storage *Adv. Mater.* **24** 5166–80
- [13] Aziz A, Zhang T, Lin Y-H, Daneshvar F, Sue H-J and Welland M E 2017 1D copper nanowires for flexible printable electronics and high ampacity wires *Nanoscale* **9** 13104–11
- [14] Liu Y, Cao X, Jiang D, Jia D and Liu J 2018 Hierarchical CuO nanorod arrays *in situ* generated on three-dimensional copper foam via cyclic voltammetry oxidization for high-performance supercapacitors *J. Mater. Chem. A* **6** 10474–83
- [15] Xu P, Liu J, Liu T, Ye K, Cheng K, Yin J, Cao D, Wang G and Li Q 2016 Preparation of binder-free CuO/Cu₂O/Cu composites: a novel electrode material for supercapacitor applications *RSC Adv.* **6** 28270–8
- [16] Chen L, Zhang Y, Zhu P, Zhou F, Zeng W, Lu D D, Sun R and Wong C 2015 Copper salts mediated morphological transformation of Cu₂O from cubes to hierarchical flower-like or microspheres and their supercapacitors performances *Sci. Rep.* **5** 9672
- [17] Kim D-W, Rhee K-Y and Park S-J 2012 Synthesis of activated carbon nanotube/copper oxide composites and their electrochemical performance *J. Alloys Compd* **530** 6–10
- [18] Liu Y, Huang H and Peng X 2013 Highly enhanced capacitance of CuO nanosheets by formation of CuO/SWCNT networks through electrostatic interaction *Electrochim. Acta* **104** 289–94
- [19] Senthilkumar V, Kim Y S, Chandrasekaran S, Rajagopalan B, Kim E J and Chung J S 2015 Comparative supercapacitance performance of CuO nanostructures for energy storage device applications *RSC Adv.* **5** 20545–53
- [20] Moosavifard S E, El-Kady M F, Rahmanifar M S, Kaner R B and Mousavi M F 2015 Designing 3D highly ordered nanoporous CuO electrodes for high-performance asymmetric supercapacitors *ACS Appl. Mater. Interfaces* **7** 4851–60
- [21] Meng F-L, Zhong H-X, Zhang Q, Liu K-H, Yan J-M and Jiang Q 2017 Integrated Cu₃N porous nanowire array electrode for high-performance supercapacitors *J. Mater. Chem. A* **5** 18972–6
- [22] Li X, Hao C, Tang B, Wang Y, Liu M, Wang Y, Zhu Y, Lu C and Tang Z 2017 Supercapacitor electrode materials with hierarchically structured pores from carbonization of MWCNTs and ZIF-8 composites *Nanoscale* **9** 2178–87
- [23] Zhang X, Shi W, Zhu J, Kharistal D J, Zhao W, Lalia B S, Hng H H and Yan Q 2011 High-power and high-energy-density flexible pseudocapacitor electrodes made from porous CuO nanobelts and single-walled carbon nanotubes *ACS Nano* **5** 2013–9
- [24] Zhang W, Yin Z, Chun A, Yoo J, Diao G, Kim Y S and Piao Y 2016 Rose rock-shaped nano Cu₂O anchored graphene for high-performance supercapacitors via solvothermal route *J. Power Sources* **318** 66–75
- [25] Dong C, Wang Y, Xu J, Cheng G, Yang W, Kou T, Zhang Z and Ding Y 2014 3D binder-free Cu₂O@Cu nanoneedle arrays for high-performance asymmetric supercapacitors *J. Mater. Chem. A* **2** 18229–35
- [26] Daneshvar-Fatah F, Wang C and Shaw L 2015 Synthesis of graphene-supported nano-Na₃MnCO₃PO₄ for high rate and high capacity sodium ion batteries *ECS Meeting Abstracts* pp 12–12
- [27] Lee C Y, Tsai H M, Chuang H J, Li S Y, Lin P and Tseng T Y 2005 Characteristics and electrochemical performance of supercapacitors with manganese oxide-carbon nanotube nanocomposite electrodes *J. Electrochem. Soc.* **152** A716–20
- [28] Fisher R A, Watt M R and Ready W J 2013 Functionalized carbon nanotube supercapacitor electrodes: a review on pseudocapacitive materials *ECS J. Solid State Sci. Technol.* **2** M3170–7
- [29] Wang K, Zhao C, Min S and Qian X 2015 Facile synthesis of Cu₂O/RGO/Ni(OH)₂ nanocomposite and its double synergistic effect on supercapacitor performance *Electrochim. Acta* **165** 314–22
- [30] Zhi M, Xiang C, Li J, Li M and Wu N 2013 Nanostructured carbon-metal oxide composite electrodes for supercapacitors: a review *Nanoscale* **5** 72–88
- [31] Sugimoto W, Shibutani T, Murakami Y and Takasu Y 2002 Charge storage capabilities of rutile-type RuO₂-VO₂ solid solution for electrochemical supercapacitors *Electrochim. Solid-state Lett.* **5** A170–2
- [32] Jayalakshmi M, Rao M M, Venugopal N and Kim K-B 2007 Hydrothermal synthesis of SnO₂-V₂O₅ mixed oxide and electrochemical screening of carbon nano-tubes (CNT), V₂O₅, V₂O₅-CNT, and SnO₂-V₂O₅-CNT electrodes for supercapacitor applications *J. Power Sources* **166** 578–83
- [33] Shakir I, Ali Z, Bae J, Park J and Kang D J 2014 Layer by layer assembly of ultrathin V₂O₅ anchored MWCNTs and graphene on textile fabrics for fabrication of high energy density flexible supercapacitor electrodes *Nanoscale* **6** 4125–30
- [34] Ramani M, Haran B S, White R E, Popov B N and Arsov L 2001 Studies on activated carbon capacitor materials loaded with different amounts of ruthenium oxide *J. Power Sources* **93** 209–14

- [35] Sun D, Everett W N, Chu C C and Sue H J 2009 Single-walled carbon-nanotube dispersion with electrostatically tethered nanoplatelets *Small* **5** 2692–7
- [36] Daneshvar-Fatah F and Nasirpouri F 2014 A study on electrodeposition of Ni-noncovalently treated carbon nanotubes nanocomposite coatings with desirable mechanical and anti-corrosion properties *Surf. Coat. Technol.* **248** 63–73
- [37] Okpalugo T I T, Papakonstantinou P, Murphy H, McLaughlin J and Brown N M D 2005 High resolution XPS characterization of chemical functionalised MWCNTs and SWCNTs *Carbon* **43** 153–61
- [38] Kundu S, Wang Y, Xia W and Muhler M 2008 Thermal stability and reducibility of oxygen-containing functional groups on multiwalled carbon nanotube surfaces: a quantitative high-resolution xps and TPD/TPR study *J. Phys. Chem. C* **112** 16869–78
- [39] Abdelkader A, Kinloch I and Dryfe R 2014 High-yield electro-oxidative preparation of graphene oxide *Chem. Commun.* **50** 8402–4
- [40] Pan H, Poh C K, Feng Y P and Lin J 2007 Supercapacitor electrodes from tubes-in-tube carbon nanostructures *Chem. Mater.* **19** 6120–5
- [41] An G, Na N, Zhang X, Miao Z, Miao S, Ding K and Liu Z 2007 SnO₂/carbon nanotube nanocomposites synthesized in supercritical fluids: highly efficient materials for use as a chemical sensor and as the anode of a lithium-ion battery *Nanotechnology* **18** 435707
- [42] Hussain Z, Salim M A, Khan M A and Khawaja E E 1989 X-ray photoelectron and auger spectroscopy study of copper-sodium-germanate glasses *J. Non-Cryst. Solids* **110** 44–52
- [43] Baddorf A P and Wendelken J F 1991 High coverages of oxygen on Cu(110) investigated with XPS, LEED, and HREELS *Surf. Sci.* **256** 264–71
- [44] Jolley J G, Geesey G G, Hankins M R, Wright R B and Wichlacz P L 1989 Auger electron and x-ray photoelectron spectroscopic study of the biocorrosion of copper by alginic acid polysaccharide *Appl. Surf. Sci.* **37** 469–80
- [45] Yu Z, Tetard L, Zhai L and Thomas J 2015 Supercapacitor electrode materials: nanostructures from 0 to 3 dimensions *Energy Environ. Sci.* **8** 702–30
- [46] Cetinkaya T, Uysal M, Guler M O, Akbulut H and Alp A 2014 Improvement cycleability of core-shell silicon/copper composite electrodes for Li-ion batteries by using electroless deposition of copper on silicon powders *Powder Technol.* **253** 63–9
- [47] Lang X, Hirata A, Fujita T and Chen M 2011 Nanoporous metal/oxide hybrid electrodes for electrochemical supercapacitors *Nat. Nanotechnol.* **6** 232
- [48] Zhang L, Tang C and Gong H 2014 Temperature effect on the binder-free nickel copper oxide nanowires with superior supercapacitor performance *Nanoscale* **6** 12981–9
- [49] Yu L, Jin Y, Li L, Ma J, Wang G, Geng B and Zhang X 2013 3D porous gear-like copper oxide and their high electrochemical performance as supercapacitors *Cryst. Eng. Comm.* **15** 7657–62
- [50] Li Y, Chang S, Liu X, Huang J, Yin J, Wang G and Cao D 2012 Nanostructured CuO directly grown on copper foam and their supercapacitance performance *Electrochim. Acta* **85** 393–8
- [51] Velmurugan V, Srinivasarao U, Ramachandran R, Saranya M and Grace A N 2016 Synthesis of tin oxide/graphene (SnO₂/G) nanocomposite and its electrochemical properties for supercapacitor applications *Mater. Res. Bull.* **84** 145–51
- [52] Prasad K R and Miura N 2004 Electrochemical synthesis and characterization of nanostructured tin oxide for electrochemical redox supercapacitors *Electrochem. Commun.* **6** 849–52
- [53] Li F, Song J, Yang H, Gan S, Zhang Q, Han D, Ivaska A and Niu L 2009 One-step synthesis of graphene/SnO₂ nanocomposites and its application in electrochemical supercapacitors *Nanotechnology* **20** 455602
- [54] Lim S, Huang N and Lim H 2013 Solvothermal synthesis of SnO₂/graphene nanocomposites for supercapacitor application *Ceram. Int.* **39** 6647–55
- [55] Hwang S-W and Hyun S-H 2007 Synthesis and characterization of tin oxide/carbon aerogel composite electrodes for electrochemical supercapacitors *J. Power Sources* **172** 451–9
- [56] Shinde S K, Dubal D P, Ghodake G S and Fulari V J 2015 Hierarchical 3D-flower-like CuO nanostructure on copper foil for supercapacitors *RSC Adv.* **5** 4443–7
- [57] Grugeon S, Laruelle S, Herrera-Urbina R, Dupont L, Poizot P and Tarascon J M 2001 Particle size effects on the electrochemical performance of copper oxides toward lithium *J. Electrochem. Soc.* **148** A285–92
- [58] Chen W, Fan Z, Gu L, Bao X and Wang C 2010 Enhanced capacitance of manganese oxide via confinement inside carbon nanotubes *Chem. Commun.* **46** 3905–7
- [59] Zhang H, Song H, Chen X and Zhou J 2012 Enhanced lithium ion storage property of Sn nanoparticles: the confinement effect of few-walled carbon nanotubes *J. Phys. Chem. C* **116** 22774–9
- [60] Chen W, Pan X, Willinger M-G, Su D S and Bao X 2006 Facile autoreduction of iron oxide/carbon nanotube encapsulates *J. Am. Chem. Soc.* **128** 3136–7
- [61] Ng M-F, Zheng J and Wu P 2010 Evaluation of Sn nanowire encapsulated carbon nanotube for a Li-ion battery anode by DFT calculations *J. Phys. Chem. C* **114** 8542–5
- [62] Yu C, Masarapu C, Rong J, Wei B and Jiang H 2009 Stretchable supercapacitors based on buckled single-walled carbon-nanotube macrofilms *Adv. Mater.* **21** 4793–7
- [63] Wang G, Huang J, Chen S, Gao Y and Cao D 2011 Preparation and supercapacitance of CuO nanosheet arrays grown on nickel foam *J. Power Sources* **196** 5756–60
- [64] Hu C-C, Wang C-C and Chang K-H 2007 A comparison study of the capacitive behavior for sol-gel-derived and co-annealed ruthenium-tin oxide composites *Electrochim. Acta* **52** 2691–700